DOI: 10.1002/ejic.201100130

Thermal Stability of High Performance Thermoelectric β-Zn_4Sb_3 in Argon

Hao Yin,[a] Birgitte L. Pedersen,[a] and Bo B. Iversen*[a]

Keywords: Zinc / Antimony / Thermoelectric materials / Thermal stability / Synchrotron diffraction

The stability of the high performance thermoelectric β-Zn_4Sb_3 is investigated by multi-temperature high resolution synchrotron powder X-ray diffraction. Contrary to previous claims β-Zn_4Sb_3 is not stable when heated in argon and degradation is observed already at 500 K. Nevertheless, the thermal stability of β-Zn_4Sb_3 is much improved in argon (ca. 5 wt.-% degradation after three heating cycles to 625 K) relative to heating in atmospheric air (ca. 60 wt.-% degradation). Based on identification of the decomposition products two specific degradation processes are proposed, and the excellent stability of β-Zn_4Sb_3 synthesized by zone melting (equilibrium method) is discussed in relation to the poor stability of material synthesized by thermal quenching (non-equilibrium process). The room temperature peak widths and unit cell parameters change significantly after three heating cycles to 625 K suggesting that the β-Zn_4Sb_3 phase diagram could be more complex than currently believed.

Introduction

Increasing pressure on the environment and the energy supply has revived interest in the search for more efficient thermoelectric materials. The β-phase of Zn_4Sb_3 has been found to be an excellent *p*-type thermoelectric semiconductor when used in the intermediate temperature range (473–673 K).[1] The thermoelectric figure of merit is defined as $zT = S^2\sigma T/\kappa$, where S is the thermopower, σ the electrical conductivity, κ the thermal conductivity ($\kappa_{lattice} + \kappa_{electronic}$) and T the absolute temperature. Good thermoelectric materials are typically strongly doped semiconductors with complex structures and large unit cells, which favor the preservation of a high power factor ($S^2\sigma$), while various phonon scattering processes lowers the thermal conductivity.[2–5] It is three disordered interstitial Zn sites which endow β-Zn_4Sb_3 an unusually low thermal conductivity and makes it a competitive thermoelectric candidate.[3] β-Zn_4Sb_3 has received considerable interest also because it is among the cheapest thermoelectric materials known, and it is made of non-toxic elements.[6–8] However, the real thermoelectric performance of Zn_4Sb_3 can be difficult to assess because the material decomposes in the expected working temperature range.[1,5,9] Thermal stability of a material is a prerequisite for being able to define a proper material zT value. If a material decomposes during measurement of the properties then clearly the "zT value" will not relate to the specific material and it will give limited information about the potential thermoelectric performance of the compound. The situation gets even more problematic in practice, because the individual parameters of zT typically are measured separately and often on different samples. The latter in itself introduces a systematic bias, but if the material is not thermally stable then multiplication of the individually measured values of S, σ, and κ has limited use.

β-Zn_4Sb_3 was originally reported to be stable up to 673 K in argon, and up to 523 K in dynamic vacuum.[1,2] When held at elevated temperatures, the compound partly decomposed but the specific products and quantitative degree of the decomposition were not reported. The originally reported thermal stability has been questioned by several authors. They found that β-Zn_4Sb_3 starts to decompose at temperatures below the expected temperature,[9] by losing Zn,[10] and forming ZnSb and Zn as decompositon products.[5] Iversen and co-workers reported the instability of the material even below 500 K with formation ZnSb, ZnO and elemental Sb as degradation products.[11] An onset temperature of 469 K was reported by Erk et al. in the study of metastable nanocrystalline Zn_4Sb_3.[12] It has been shown that β-Zn_4Sb_3 synthesised by thermal quenching decomposes very substantially when heated in atmospheric air,[11] whereas material synthesised by zone melting exhibits a remarkable stability.[11,13] Since the properties of β-Zn_4Sb_3 synthesized by thermal quenching and by zone melting are different, it follows that the crystal structures and/or microstructure of the two materials must be different. The decomposition in air is problematic if the material is to be used in an actual thermoelectric device, but the reported zT values could still be valid since high temperature properties typically are measured in argon or vacuum. Clearly, it is important for the understanding of β-Zn_4Sb_3 that the thermal stability of the structure is established during heating

[a] Centre for Materials Crystallography, Department of Chemistry and iNANO, University of Aarhus,
140 Langelandsgade, 8000 Aarhus, Denmark
Fax: +45-86196199
E-mail: bo@chem.au.dk

Supporting information for this article is available on the WWW under http://dx.doi.org/10.1002/ejic.201100130.

in argon. It should also be mentioned that doping of Zn_4Sb_3 has been shown by Iversen et al. as a way to improve the stability.[14,15] In the present work, we study the degradation behavior of quench synthesised β-Zn_4Sb_3 by heating the sample in argon atmosphere while measuring high resolution synchrotron powder X-ray diffraction (PXRD) data.

Results and Discussion

Selected crystallographic parameters are listed in Table 1 for the data recorded at 300 K before and after heating. Even with a third-generation synchrotron source, which routinely makes crystalline phases down to a 0.1 wt.-% level detectable,[16] no impurities were observed in both samples before heating. The refined stoichiometries of the two samples are $Zn_{38.6}Sb_3$ and $Zn_{38.3}Sb_3$ for Air and Ar sample, respectively.

Table 1. Crystallographic details and refinement residuals for the sample heated in argon (Ar) and in air (Air). "start" refers to refinement of the data set recorded before heating, and "after" refers to refinement of the data set recorded at 300 K after three heating cycles.

	Ar, start	Air, start	Ar, after	Air, after
T /K	300	300	300	300
t_{exp} /min	5	5	5	5
Points	7861	7507	7867	7507
Reflections	5217	4863	5164	4682
Parameters	78	90	97	116
R_F /%	1.58	1.34	2.64	2.83
R_{Bragg} /%	1.84	1.84	2.65	2.71
R_p /%	2.85	2.39	3.62	4.06
R_{wp} /%	3.94	3.15	4.79	6.16
χ^2	6.63	2.91	8.09	12.50
$a = b$ /Å	12.2183(2)	12.2257(1)	12.2329(2)	12.2383(2)
c /Å	12.4044(2)	12.4162(1)	12.4249(2)	12.4256(2)
X	0.193(4)	0.241(4)	0.122(3)	0.218(4)
Y	0.013(0)	0.023(4)	0.005(0)	0.0001(0)
B_{iso} Sb1	1.13(3)	1.26(2)	0.98(3)	1.01(5)
B_{iso} Sb2	1.00(3)	1.25(3)	0.92(3)	0.94(6)
B_{iso} Zn	2.04(6)	2.11(5)	2.10(5)	2.11(11)
Occ Sb1	1	1	1	1
Occ Sb2	1	1	1	1
Occ Zn1	0.941(4)	0.905(3)	0.951(3)	0.944(7)
Occ Zn2	0.049(2)	0.052(1)	0.057(2)	0.065(4)
Occ Zn3	0.031(2)	0.047(2)	0.028(2)	0.034(5)
Occ Zn4	0.038(2)	0.032(1)	0.046(2)	0.045(4)
V /Å^3	1603.7(0)	1607.2(3)	1610.2(0)	1611.7(4)
Wt.-% ZnSb	0	0	2.9(1)	4.0(2)
Wt.-% ZnO	0	0	0	21.1(4)
Wt.-% Sb	0	0	2.6(0)	32.3(2)

Further details of the multi-temperature refinement are provided in Supporting Information for both samples.

The synchrotron powder diffraction patterns of the two samples, before and after heating to 625 K in the different atmospheres are shown in Figure 1. The difference in thermal behaviors is notable. A large number of additional peaks appear in the sample heated in air, and these are identified by the Rietveld refinement to be the decomposition products: ZnSb, ZnO and elemental Sb (details are shown in Table 1). In contrast, the patterns from the sample heated in argon are similar and only a couple of additional impurities peaks appear after heating. This directly shows that the degradation is much more limited for the sample heated in an inert atmosphere. Figure 2(a) plots the weight fraction of the starting phases as determined by Rietveld refinement during the first heating (300→625 K) of the two samples. It is clearly seen that both samples start to decompose before 500 K, and in the sample heated in air almost 4% of original phase has been lost at 500 K. Further heating accelerates the degradation, and only 65 wt.-% Zn_4Sb_3 is left at 625 K generating about 20 wt.-% Sb, ca. 10 wt.-% ZnO and ca. 5 wt.-% ZnSb as decomposition products, see Figure 2 (b).

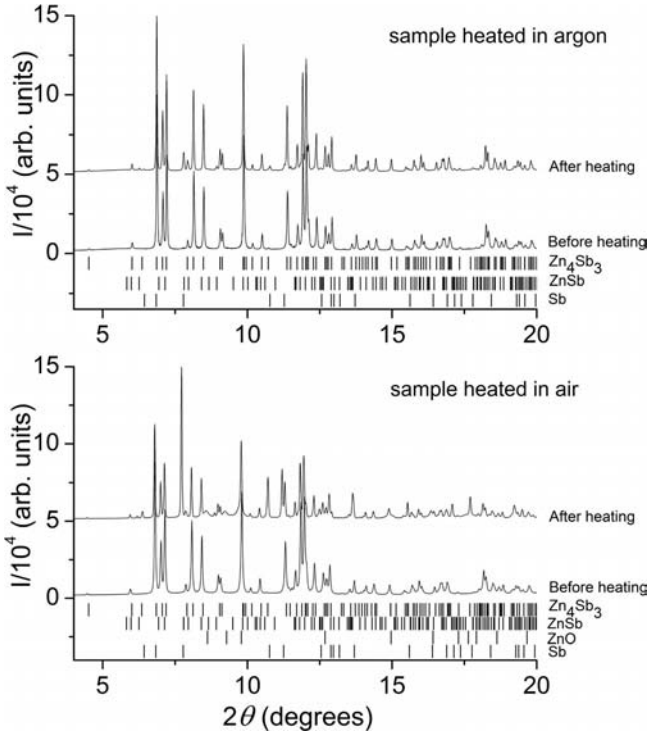

Figure 1. Powder patterns of Zn_4Sb_3 heated in argon (above) and heated in air (below) recorded at 300 K before heating, and after three heating cycles. The vertical lines correspond to the position of Bragg peaks of corresponding phases.

The decomposition behavior of the sample heated in argon is very different, see Figure 2 (a). A slight weight loss occurs below 500 K, followed by continuous but limited decomposition, of which the rate seems to decrease. At 625 K more than 96 wt.-% of the starting Zn_4Sb_3 material remains. Iversen et al.[11] studied a zone-melted Zn_4Sb_3 sample, which was found to be stable within 300 K to 625 K except for an isolated event at ca. 523 K, where a subtle decomposition is observed. Here, we observe a continuous degradation during the temperature range under study, corroborating that the thermal behavior of Zn_4Sb_3 is affected by synthesis methods. As expected, no oxidation impurities appear during the decomposition in argon, and the decomposition products are ZnSb and elemental Sb, see Figure 2 (b). However, these two products are incompatible with the stoichiometry. Additional elemental Zn, or other Zn com-

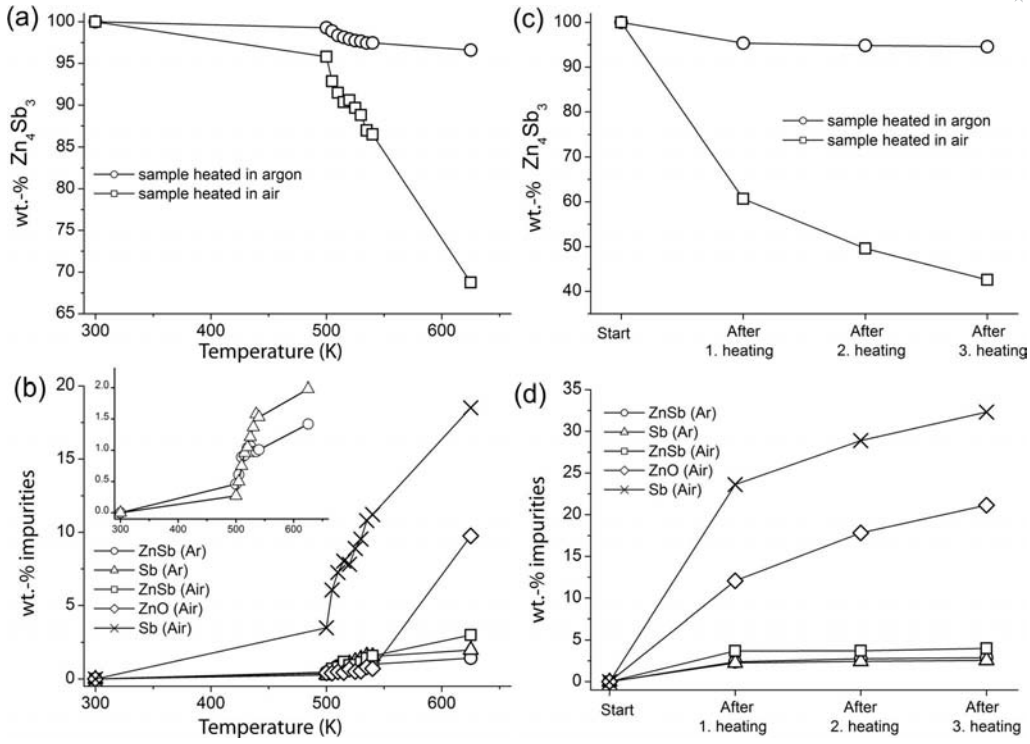

Figure 2. a) Weight fraction of remaining Zn_4Sb_3 as a function of temperature in the first heating cycle. b) Weight fraction of impurity phases ZnSb, (ZnO) and Sb as a function of temperature in the first heating cycle. c) Weight fraction of remaining Zn_4Sb_3 as a function of heating cycles. d) Weight fraction of impurity phases ZnSb, (ZnO) and Sb, as a function of heating cycles.

pounds, must form when the 4:3 phase degrades into the 1:1 phase and elemental Sb. As the capillaries were sealed, no substances can escape and it appears that the missing Zn must be present either in an undetected amorphous phase or disappear due to sublimation.

Part c of Figure 2 shows the weight fraction of the remaining Zn_4Sb_3 phase in both samples determined at 300 K after each of the three heating cycles. The sample heated in air seems to continue degrading during the first cooling down to 300 K and an additional ca. 5 wt.-% of the original phase is lost. Additional heating causes further decomposition leaving only ca. 40 wt.-% Zn_4Sb_3 after three cycles. The sample heated in argon is much more stable than that heated in air and the decomposition rate indeed is small. More than 94 wt.-% of the starting phase is still remaining after three heating cycles, and it appears that during further heating cycles Zn_4Sb_3 will reach a "plateau" of decomposition. The refined weight fractions of decomposition impurities for both samples are shown in Figure 2 (d). For a sample synthesized by zone melting the corresponding weight percentages were 4.8% ZnSb, 2.5% ZnO and 1.6% Sb,[11] while for a 1% Cd-doped sample synthesized by the quench method the weight percentages were 4.5% ZnSb, 8.4% ZnO and 8.8% Sb. (Both samples had the same thermal cycling in atmospheric air as in the present study.[15]) For the three pure Zn_4Sb_3 samples the amounts of ZnSb are similar, whereas the amounts of ZnO and Sb are distinctly different. ZbSb is stable up to at least 800 K according to the phase diagrams.[17,18] This implies that the decomposition of Zn_4Sb_3 actually consists of two different processes i. $Zn_4Sb_3 \rightarrow ZnSb + Zn$, and ii. $Zn_4Sb_3 \rightarrow Zn + Sb$. The first process (giving rise to ZnSb) occurs to approximately the same extent for all four samples independent of the atmosphere, synthesis method or doping, and this degradation therefore appears to be "intrinsic" to the structure. In molar terms 3.2% of the initial Zn_4Sb_3 degrades to ZnSb for the quench sample in argon, 4.4% of the quench sample in air, 5.3% of the zone-melted sample in air, and 5.0% of the Cd-doped quench sample heated in air. The extent of the second reaction (monitored by the Sb content) is very different in the four cases. For the pure sample heated in argon an additional 4.4 mol-% Zn_4Sb_3 degrades (into Zn and Sb), whereas 55.4% degrades during heating of the pure quench samples in air. Thus, when Zn is removed from the matrix by reaction with oxygen a very strong decomposition takes place. The corresponding number for reaction 2 for the zone melted sample heated in air is 2.8%, and it is 15.2% for the Cd-doped quench sample heated in air. The major improvement of the zone melted pure sample relative to the quench sample is the suppression of reaction 2 even in an oxygen rich atmosphere, and it only occurs to the same extent as for the sample heated in argon (3–4%). This suggests that the generated Zn atoms are not able to escape to the surface of the crystallites and get exposed to oxygen. This may be due to the fewer defects in the zone-melted sample since zone-melting is an equilibrium process, during which crystals gain more perfect lattices. A tracer diffusion study shows that Zn is highly mobile in the structure.[19] Defects should make it easier for Zn atoms to diffuse. The extent of reaction 2 is also greatly suppressed for Cd-doped sam-

ples with a decrease in Zn_4Sb_3 decomposition from 55.4% to 15.2%. This is believed to be attributed to the bigger and heavier Cd atoms acting as stabilizers to the structure blocking against Zn diffusion in the lattice. The analysis shows that generation of Zn is common to both reactions, and thus one would predict that addition of Zn to the Zn_4Sb_3 matrix should reduce the decomposition and this has indeed been observed.[13]

The room temperature unit cell parameters and the peak width (FWHM) of the (300) reflection indexed in the β-Zn_4Sb_3 phase for samples heated in argon and in air after each heating cycles are plotted in Figure 3.

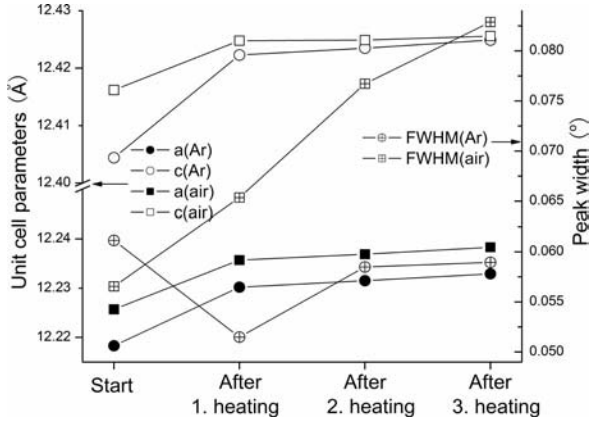

Figure 3. The changes of unit cell parameters (left axis) and peak width (FWHM) of reflection (300) indexed in Zn_4Sb_3 (right axis) against heating cycles. The estimated standard uncertainty of each unit cell parameter is below 0.0002 Å.

Since the peak profile was described by a combination of Gaussian and Lorentzian functions, the FWHM were calculated by[20]

$$FWHM^5 = H_G^5 + 2.69269H_G^4H_L + 2.42843H_G^3H_L^2 + 4.47163H_G^2H_L^3 + 0.07842H_GH_L^4 + H_L^5$$

where H_G and H_L are the individual Gaussian and Lorentzian $FWHM$ components. They are given by the expressions

$$H_G^2 = U \cdot \tan^2\theta + V \cdot \tan\theta + W$$

$$H_L = X \cdot \tan\theta + Y/\cos\theta$$

and the parameters U, V, W, X, Y are obtained from the Rietveld refinement. Before heating, the values of the unit cell parameters are a = 12.2183(2) Å, c = 12.4044(2) Å and a = 12.2257(2) Å, c = 12.4162(2) Å for the argon and the air samples, respectively. These values are comparable to our previous studies and to the values reported by Snyder et al., which were based on similar data as the present.[3,11] However, they are lower than those reported by other authors based on different types of data.[21,22,23] When the samples are heated to 625 K and then cooled to room temperature, the unit cell parameters increase monotonously. After three heating cycles to 625 K, the increase in the room temperature unit cell parameters levels off. In principle, the unit cell parameters of the two samples should be identical before the start of the experiments, since the samples were from the same synthesis batch and underwent similar preparation. Despite of the systematic error between the two data sets, it appears that the relative change for both samples is clear (ca. 0.01 Å compared with an estimated standard uncertainty of ca. 0.0002 Å), and that the unit cell parameters increase with thermal cycling.

The behaviour of the peak width is quite different for the samples heated in air and in argon. For the sample heated in air there is a significant increase in peak width, which appears to continue with further heating cycles. On the other hand, for the sample heated in argon the behaviour is tricky. The peak width first decreases after one heating cycle, and during the two subsequent cycles increases back to near the starting value. The changes in unit cell parameters and peak widths of β-Zn_4Sb_3 indicate that not only does the material decompose, but the crystal structure and/or microstructure of the phase itself changes. The peak broadening and unit cell changes could in reality mask that distinct new phases with very similar unit cell parameters are formed from the parent phase. Further investigations are needed to clarify if this is the case.

Conclusions

In summary, it is found that β-Zn_4Sb_3 is not as previously reported stable during heating in argon. Based on identification of the decomposition products from different β-Zn_4Sb_3 samples heated in air and in argon it is proposed that the degradation of Zn_4Sb_3 consists of two processes: i. $Zn_4Sb_3 \rightarrow 3\ ZnSb + Zn$, and ii. $Zn_4Sb_3 \rightarrow 4\ Zn + 3\ Sb$. Reaction 1 relates to the thermodynamic stability of Zn_4Sb_3, while the oxidation of Zn accelerates reaction 2, and in the case of samples synthesized by thermal quenching the decomposition is more than 55% for samples heated in air. In terms of practical use, it has empirically been observed that the decomposition is suppressed if pellets synthesized by the quench method are hot-pressed with additional Zn. The two proposed decomposition reactions give a clear explanation for this fact. Due to the severe decomposition material synthesized by thermal quenching must be isolated from oxygen e.g. by coating the legs of the device or protecting the entire module. Material synthesized by zone melting has a strong suppression of reaction 2, which means that it does not suffer from the presence of oxygen. However, such material still benefits from additional Zn during pressing to suppress reaction 1. Since β-Zn_4Sb_3 is shown not to be stable even at temperatures much below the β-γ phase boundary, reports of zT values of β-Zn_4Sb_3 must be interpreted with care. A material zT value is only really meaningful for materials which are stable, i.e. materials which preserve their identity during the measurement of their properties.

Experimental Section

Synthesis and Sample Preparation: Approximately 70 g of Zn_4Sb_3 was prepared by mixing stoichiometric amounts of 99.99% Zn

shots and 99.5% Sb powder in a quartz ampule. The vacuum sealed ampule was placed horizontally into a tube furnace and heated to 973 K with a 400 K/h ramp under continuous rotation for 2 h before quenching in ice water. The resulting polycrystalline, rod shaped sample was ground in an agate mortar and sieved to obtain a grain size less than 45 μm. Homogenous grain size powder, which is important for synchrotron powder diffraction measurement, was obtained by a floating technique. The powders were floated with ethyl alcohol in a Petri dish and left for sedimentation. After 1 min, the top layer of the ethanol was transferred into a new Petri dish, and left for another 1 min for further sedimentation. The top layer was then again moved to a third Petri dish and the ethanol was evaporated, leaving a sample fraction of homogeneous grain size. The samples were filled into 0.2 mm capillaries, followed by about 5 min ultra-sound bath to obtain a dense packing. One capillary was sealed under open air while the other was sealed with epoxy in an argon filled glove box.

Multitemperature Synchrotron PXRD Recording: Multi-temperature, high resolution synchrotron PXRD data were recorded using the large Debye–Scherrer camera at beam line BL02B2, SPring8, Japan.[24] The data were measured at λ = 0.42236(1) and 0.42282(0) Å for samples heated in air and in argon, respectively, using exposure times of 5 min. The wavelengths were determined from refinements on a CeO_2 standard. Data were collected at 300 K, between 500–540 K with a step width of 5 K, and at 625 K. After the first heating, the samples were cooled down to 300 K and heated again for another two cycles (i.e. the thermal history was 300→625→300→625→300→625→300 K) to imitate a practical application. All data sets were Rietveld refined against the crystal structure model of Snyder et al.[3] with the program FULLPROF.[25] Data outside the Bragg angle range $3° < 2\theta < 40°$ were excluded because of low signal-background ratio. A Pseudo-Voigt function with three Gaussian, two Lorentzian, and two asymmetry parameters was found to give a good description of the peak profile, while the background was fitted by linear interpolation among approximately 60 points.

Supporting Information (see footnote on the first page of this article): Selected crystallographic details and unit cell parameters for Zn_4Sb_3 heated in argon, derived from Rietveld refinement are shown in Table ST1, ST2. Selected crystallographic details and unit cell parameters for Zn_4Sb_3 heated in air, derived from Rietveld refinement are shown in Table ST3, ST4.

Acknowledgments

This work was supported by the Danish National Research Foundation (Center for Materials Crystallography), the Danish Strategic Research Council (Center for Energy Materials), and the Danish Research Council for Nature and Universe (Danscatt). The synchrotron radiation experiment at the SPring-8 synchrotron was conducted with the approval of the Japan Synchrotron Radiation Research Institute.

[1] T. Caillat, J.-P. Fleurial, A. Borshchevsky, *J. Phys. Chem. Solids* **1997**, *58*, 1119–1125.
[2] T. Caillat, A. Borshchevsky and J.-P. Fleurial, US Patent 6942728 B2 **2005**.
[3] G. J. Snyder, M. Christensen, E. Nishibori, T. Caillat, B. B. Iversen, *Nat. Mater.* **2004**, *3*, 458–463.
[4] F. Cargnoni, E. Nishibori, P. Rabiller, L. Bertini, G. J. Snyder, M. Christensen, C. Gatti, B. B. Iversen, *Chem. Eur. J.* **2004**, *10*, 3861–3870.
[5] Y. Mozharivskyj, Y. Janssen, J. L. Harringa, A. Kracher, A. O. Tsokol, G. J. Miller, *Chem. Mater.* **2006**, *18*, 822–831.
[6] L. Pan, X. Y. Qin, H. X. Xin, D. Li, J. H. Sun, J. Zhang, C. J. Song, R. R. Sun, *Intermetallics* **2010**, *18*, 1106–1110.
[7] J. Nylen, M. Andersson, S. Lidin, U. Haussermann, *J. Am. Chem. Soc.* **2004**, *126*, 16306–16307.
[8] S.-C. Ur, P. Nash, R. Schwarz, *Met. Mater. Int.* **2005**, *11*, 435–441.
[9] L. T. Zhang, M. Tsutsui, K. Ito, M. Yamaguchi, *J. Alloys Compd.* **2003**, *358*, 252–256.
[10] Y. Mozharivskyj, A. O. Pecharsky, S. Bud′ko, G. J. Miller, *Chem. Mater.* **2004**, *16*, 1580–1589.
[11] B. L. Pedersen, B. B. Iversen, *Appl. Phys. Lett.* **2008**, *92*, 161907-161907-3.
[12] S. Schlecht, C. Erk, M. Yosef, *Inorg. Chem.* **2006**, *45*, 1693–1697.
[13] B. B. Iversen, B. Lundtoft, M. Christensen, D. Platzek, Patent WO 128467 A2 **2006**.
[14] B. L. Pedersen, H. Birkedal, E. Nishibori, A. Bentien, M. Sakata, M. Nygren, P. T. Frederiksen, B. B. Iversen, *Chem. Mater.* **2007**, *19*, 6304–6311.
[15] B. L. Pedersen, H. Yin, H. Birkedal, M. Nygren, B. B. Iversen, *Chem. Mater.* **2010**, *22*, 2375–2383.
[16] S. Johnsen, A. Bentien, G. K. H. Madsen, M. Nygren, B. B. Iversen, *Phys. Rev. B* **2007**, *76*, 245126-245126-9.
[17] Y. Liu, J.-C. Tedenac, *CALPHAD*, *Comput. Coupling Phase Diagrams Thermochem.* **2009**, *33*, 684–694.
[18] V. Izard, M. C. Record, J. C. Tedenac, S. G. Fries, *CALPHAD*, *Comput. Coupling Phase Diagrams Thermochem.* **2001**, *25*, 567–581.
[19] E. Chalfin, H. X. Lu, R. Dieckmann, *Solid State Ionics* **2007**, *178*, 447–456.
[20] P. Thompson, D. E. Cox, J. B. Hastings, *J. Appl. Crystallogr.* **1987**, *20*, 79–83.
[21] G. Nakamoto, T. Souma, M. Yamaba, M. Kurisu, *J. Alloys Compd.* **2004**, *377*, 59–65.
[22] T. Souma, M. Ohtaki, *J. Alloys Compd.* **2006**, *413*, 289–297.
[23] V. L. Kuznetsov, D. M. Rowe, *J. Alloys Compd.* **2004**, *372*, 103–106.
[24] E. Nishibori, M. Takata, K. Kato, M. Sakata, Y. Kubota, S. Aoyagi, Y. Kuroiwa, M. Yamakata, N. Ikeda, *J. Phys. Chem. Solids* **2001**, *62*, 2095–2098.
[25] J. Rodríguez-Carvajal, *FULLPROF*, **2000**, **2001**.

Received: February 7, 2011
Published Online: May 10, 2011

